An X-ray diffraction study on the temperature and chemical composition dependence of the modulation wave vector in $((CH_3)_4N)_2ZnCl_{4-x}Br_x$ compounds

1994 J. Phys.: Condens. Matter 6 8205

(http://iopscience.iop.org/0953-8984/6/40/012)

J. Phys.: Condens. Matter 6 (1994) 8205–8218. Printed in the UK

An x-ray diffraction study on the temperature and chemical composition dependence of the modulation wave vector in $[(CH_3)_4N]_2ZnCl_{4-x}Br_x$ compounds

L J P Vogels†, H Meekes† and J L de Boer‡

† R I M Laboratory of Solid State Chemistry, University of Nijmegen, Toernooiveld, 6525 ED Nijmegen, The Netherlands

‡ Materials Science Centre, Laboratory of Chemical Physics, University of Groningen, Nijenborgh 4, 9747 AG Groningen, The Netherlands

Received 13 May 1994, in final form 11 July 1994

Abstract. In this paper we study the behaviour of the modulation wave vector in $[(CH_3)_4N]_2ZnCl_{4-x}Br_x$ compounds as a function of composition (x) and temperature. We compare the results of this x-ray study with those of morphological experiments. The two results are quite well correlated, showing several lock-in phases of the modulated structure being stable over a temperature range of a few degrees. In particular, the existence of a recently found new phase with modulation wave vector $q = \frac{4}{11}c^*$ is confirmed. We also find evidence for phases with $q = \frac{10}{27}c^*$, $q = \frac{14}{37}$ (or $\frac{17}{45}$)c^*, $q = \frac{14}{39}c^*$, $q = \frac{3}{8}c^*$, $q = \frac{5}{12}c^*$, $q = \frac{13}{36}$ (or $\frac{17}{47}$)c^* and $q = \frac{5}{14}$ (or $\frac{16}{45}$)c^*. These phases are interpreted within the framework of a microscopic model.

1. Introduction

In this paper we study a so-called modulated crystal structure. Whereas classical crystal structures can be described by three periodicities (a, b, c) and a set of symmetry operators, modulated crystal structures are described by $3+d$ ($d = 1$ in the present case) periodicities [1–4]. The extra parameters are necessary to describe the periodic distortion (the modulation) of the average lattice. This distortion is described on the reciprocal lattice of the average structure by an additional wave vector q. If the modulation wave vector is a linear combination of the reciprocal basis vectors (a^*, b^* and c^*) with rational fractions, the structure is commensurate and forms in fact a superstructure, otherwise it is incommensurate. The three-dimensional crystal structure we are able to observe is then an intersection of a $3+d$-dimensional descriptive so-called superspace embedding with the three-dimensional real space.

In x-ray-diffraction experiments the presence of a modulation wave vector shows up as generally weak spots, the so-called satellite reflections, besides the main reflections. These satellite reflections can be indexed by $3+d$ integers. In the case of $d = 1$ this results in a labelling of the reflections with ($hklm$) instead of the usual (hkl). The main reflections, due to the average structure, are then labelled as ($hkl0$). The position of the satellite reflections with respect to the main reflections, which latter are due to the basic structure without a modulation, represents the modulation wave vector. Interestingly, a modulation in a crystal structure has also macroscopic effects as it influences the morphology. Satellite faces are

0953-8984/94/408205+14$19.50

formed, of which the relative orientations are directly correlated to the modulation wave vector. The normal of a face $(hklm)$ is given by $H = ha^* + kb^* + lc^* + mq$. Thus, it is possible to determine the modulation wave vector from morphological experiments [5–10].

$[(CH_3)_4N]_2ZnCl_{4-x}Br_x$ is a compound with an average β-K_2SO_4 structure [11]. $[(CH_3)_4N]_2ZnCl_{4-x}Br_x$ has many phases of which most are modulated [12–16]. The symmetry of the corresponding structures can be described to a good approximation by a single (3 + 1-dimensional) superspace group, each commensurate phase corresponding to a three-dimensional subgroup of this superspace group [6, 17, 18]. In all cases, changing the composition (x) in $[(CH_3)_4N]_2ZnCl_{4-x}Br_x$ seems to lead to stable crystallographic phases.

The phase diagram of $[(CH_3)_4N]_2ZnCl_{4-x}Br_x$ is shown in figure 1. As can be seen, for temperatures below the transition to the high-temperature (not modulated) paraphase, several incommensurate as well as commensurate regions exist (e.g. $q = \frac{1}{3}$, $\frac{2}{5}$ and $\frac{4}{11}c^*$). The magnitude and direction of the modulation wave vector q are a function of both composition x and temperature T. The behaviour of q as a function of x and T has been studied extensively by morphological experiments [9]. The results turned out to be in good agreement with the x-ray-diffraction studies of Colla [15]. As an intriguing result from the morphological study a new commensurate phase was found having a modulation wave vector $q = \frac{4}{11}c^*$ within the incommensurate phase for values of x between 1.2 and 2.2. In the phase diagram the change of composition can be interpreted as an increase of the internal pressure of the crystal, due to the substitution of chloride ions by the larger bromide ions. This change in internal pressure can be compared with the effect of an external hydrostatic pressure.

Gesi [19] gave a brief review of the interpretation of experimental results on hydrostatic pressure effecting the lock-in transitions in various tetramethylammonium tetrahalogenometallic compounds, $[N(CH_3)_4]_2XY_4$ (X: Mn, Fe, Co, Ni, Cu, Zn; Y: Cl, Br). The techniques used were neutron and x-ray diffraction, and dielectric and DTA measurements. He found that the pressure–temperature phase diagrams of the chloride compounds with X = Mn, Fe, Co and Zn can be unified in a reduced p–T diagram. In this description the phases in the -$MnBr_4$, -$CoBr_4$ and -$ZnBr_4$ compounds correspond to the high-pressure ones of the chloride compounds. The deuteration effect of the phase transition at high pressure is also discussed by this author.

In order to find an explanation for the rich phase diagram of these tetramethylammonium tetrahalogenometallic compounds as well as that of others, in terms of a microscopical model one has to realize that the structure of the ground state is characterized by commensurate and incommensurate phases, each with their own specific modulation wave vector. Such a phase diagram shows some resemblance with that obtained with the ANNNI model [20, 21] used to find the structure of a two-dimensional Ising lattice, with two interactions that are opposite in sign. Janssen and Tjon [22] used a so-called one-dimensional frustrated ϕ^4 model, which is related to the ANNNI model, to describe incommensurate and commensurate phases microscopically. The model results in ground-state configurations being a function of two parameters A' and B' (see [22] for a precise definition), which are related to the energy or temperature and the pressure parameter. Thus, a generalized phase diagram is obtained describing the ground-state configurations as a function of these parameters. The ground states of the different phases appearing are characterized by a modulation wave number, being n/m, n and m integer. If one of the parameters (A') in the model is relatively small, only two ground states are found, namely the ones with wave vector $\frac{1}{2}$ and $\frac{1}{4}$ (for a positive value of B'). If now A' increases, new phases, either commensurate or incommensurate, 'appear'. The first new commensurate phase has $n/m = \frac{1}{3}$. Then

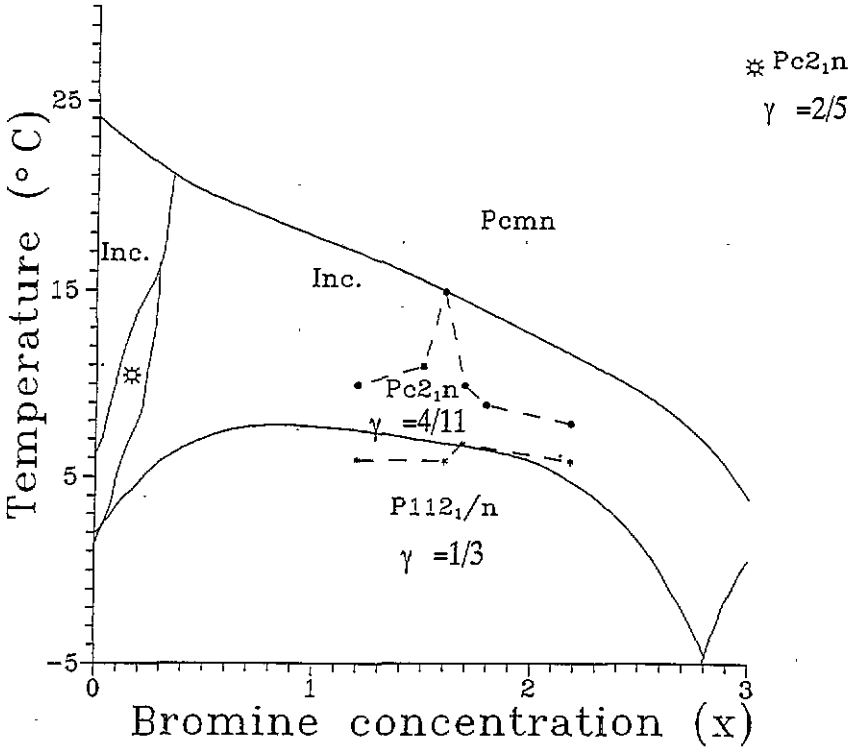

Figure 1. The phase diagram of $[(CH_3)_4N]_2ZnCl_{4-x}Br_x$ containing several commensurately and incommensurately modulated phases [9, 16]. The modulation wave-vector parameter γ and the space-group symmetry are indicated for all commensurate phases. • indicates T_i and * indicates T_c, both as determined by Vogels *et al* [9]; lines are guides to the eye.

again, additional intermediate phases occur. The different generations of new values for the modulation wave number are characterized by the so-called Farey numbers, as far as commensurate phases are concerned. Two examples of a sequence of numbers, starting with two different pairs of initial values for n/m will be given further on. It should be noted that the wave numbers are rational.

If one continues to generate Farey numbers, in the end one obtains all rational numbers lying between the two boundary values of the starting ones. Selke and Duxbury [23] showed that these limiting values for the wave numbers form a complete devil's staircase.

The aim of this paper is to report on a study of the modulation wave vector in $[(CH_3)_4N]_2ZnCl_{4-x}Br_x$ in the neighbourhood of the recently found phase in morphological experiments, with $q = \frac{4}{11}c^*$ [9], using x-ray-scattering techniques. The results will be compared with those of the morphological study and interpreted in terms of the models described above.

In the paraphase ($T > T_i$) the crystal is not modulated. The intensity of the x-ray satellite reflections in the incommensurate phase decreases as the temperature approaches that of the paraphase from below [15, 24]. This decrease is due to a decreasing amplitude of the modulation wave vector. We used this phenomenon of vanishing satellite reflections to find T_i. There is a second characteristic phase transition from the incommensurate phase to the first commensurate so-called lock-in phase at lower temperature T_c. We will use the term lock-in phase also for the transitions to other commensurate phases at even lower

temperatures.

2. Experimental details

We performed our x-ray experiments on an Enraf Nonius CAD-4 diffractometer, using dedicated software and Mo Kα radiation. Small crystals were cut from the same crystals we had used in the morphological experiments [9]. These small crystals were glued on a thin glass fibre and were encapsulated by glue to prevent condensation of water on the crystal surface. Next, we put the crystal on a goniometer head of the CAD-4. After centring the crystal we determined the reciprocal-axis matrix, the cell parameters and the standard deviations. At first, we scanned more than 900 main reflections ($hkl0$) and more than 900 corresponding first-order satellite reflections ($hklm$) with $m = 1$ and $m = -1$, to determine the most important satellite and main reflections. Using the setting for which the superspace group is $Pcmn(00\gamma)(1s-1)$ we chose the reflections of the forms {2 2 9 0}, {3 7 0 0}, {12 0 0 0}, {0 6 4 0} and {10 0 6 0} to determine the parameters of the average cell. Given these cell parameters, the reflections (1 3 1 0), (1 3 1 1), (1 3 1 −1), (−1 3 1 0), (−1 3 1 1), (−1 3 1 −1), (1 −3 1 0), (1 −3 1 1), (1 −3 1 −1), (1 3 −1 0), (1 3 −1 1), (1 3 −1 −1), (0 2 0 0), (0 2 0 1) and (0 2 0 −1) were used to determine the modulation wave vector. As far as the error in the value of the wave vector (γ) is concerned, we used the following procedure. For each composition (x) and temperature the five triplets of reflections ($hkl1$), ($hkl0$) and ($hkl-1$) were used to find five values for γ. Each triplet was chosen symmetrically around a main reflection, along the c^*-direction, thus minimizing any systematic error along the direction in which γ is determined. These five values for γ were averaged and the standard-deviation values were determined from the standard deviation of each triplet value.

Further, the relatively strong reflections (0 −1 4 0), (1 3 −1 0), (1 3 1 0), (1 3 1 1), (1 3 1 −1), (0 2 0 0), (0 2 0 1) and (0 2 0 −1) were used to determine the intensity of the reflections, where in this case the ($hkl0$) reflections functioned as a standard calibration.

We cooled the crystal with a constant air flow of 15 ml s^{-1}. We kept the gas itself at a constant temperature using a thermostatted spiralized cooling tube connected by hoses to a thermostatted water/ethanol bath (figure 2). The tube itself and the hoses leading to and from it were well isolated. The temperature of the gas flow was measured just above the crystal, using a copper–constantan thermocouple with an electronic cold-junction compensator at 0 °C and a millivoltmeter. We estimate that the temperature of the gas flow was constant within ±0.1 °C and that the absolute accuracy of the temperature measurements is ±1 °C. After stabilizing the temperature of the gas flow for about five minutes, we started our measurements, assuming that the crystal had enough time to adapt to the gas temperature, and indeed during the measurements (approximately 1 h) for which the crystal was held at the same temperature, we did not observe changes in q. Following earlier reports we investigated five compositions of $[(CH_3)_4N]_2ZnCl_{4-x}Br_x$ namely $x = 0$, 1.20, 1.60, 1.69 and 2.19 respectively [9]. For several compositions two crystals were investigated and/or two temperature runs were performed. The temperature range examined was from about −3 °C to about 25 °C.

3. Results

First we checked the behaviour of the modulation wavevector. In figure 3 we plotted the size of the modulation parameter versus temperature for the different values of $x > 0$.

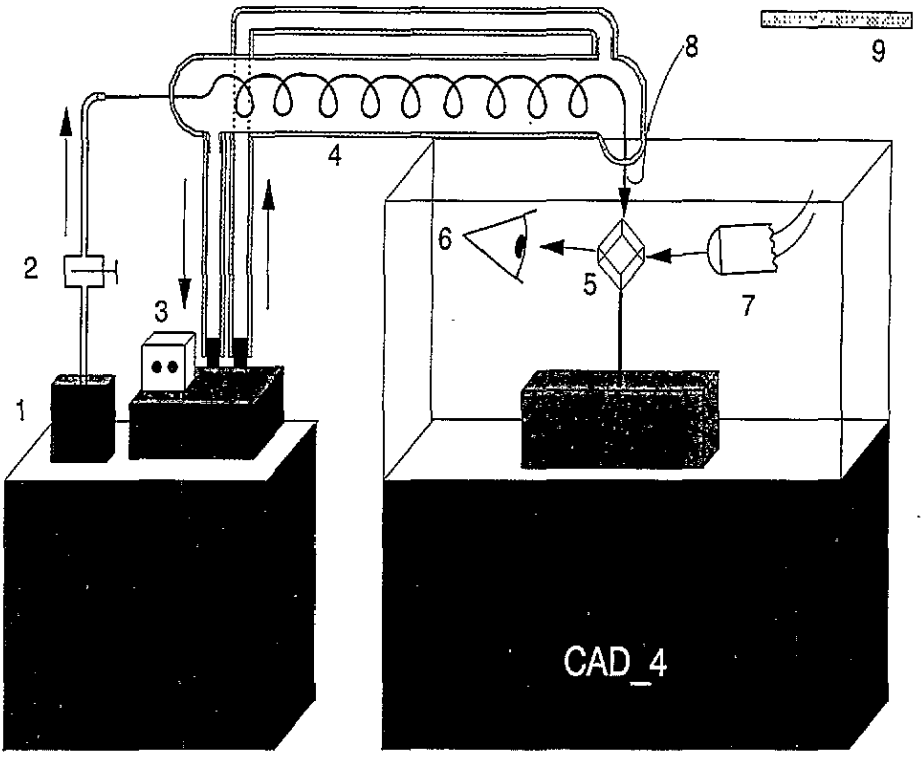

Figure 2. The experimental set-up. 1, gas pump; 2, tap/flow meter; 3, thermostat; 4, cooling tube; 5, crystal; 6, detector; 7, Mo Kα source; 8, thermocouple and 9, thermal isolation.

For $x = 0$ only three data points were determined, therefore we omitted the corresponding figure. Note that the figures are sometimes composed of more than one temperature run or crystal. In these figures we observe different plateaus. The value for γ we identify with a plateau was determined by a weighted average of the different (temperature) values. For this purpose, we gathered those values which could be averaged within their standard deviation to a single value. The error in this value of a plateau was determined from the corresponding standard-deviation values. In the following we will assign a commensurate wave number (n/m) to the observed plateau values. The choice of the commensurate value is based on the relevant Farey numbers as mentioned in the introduction and will be explained in more detail in the discussion. In table 1 we summarize the results of the values of γ for the different identified plateaus.

We now come to the results on the intensities of the different reflections. In figure 4 we plotted the intensity of different reflection spots as a function of temperature, for the different compositions. It can be seen that the intensity of the main reflections remains almost constant or increases slightly, while that of the satellite reflections decreases towards zero with increasing temperature. We note that, taking T_i as the temperature where the intensity of the satellite reflections becomes zero, T_i determined from the intensity is rather close to T_i as determined by Colla *et al* [15, 16], the latter value being depicted in the figure (see also figure 1). Note that the intensities are scaled. For some compositions the intensities of the satellite reflections remain, though being very weak, non-zero slightly above T_i, still indicating that there is at least a change at T_i.

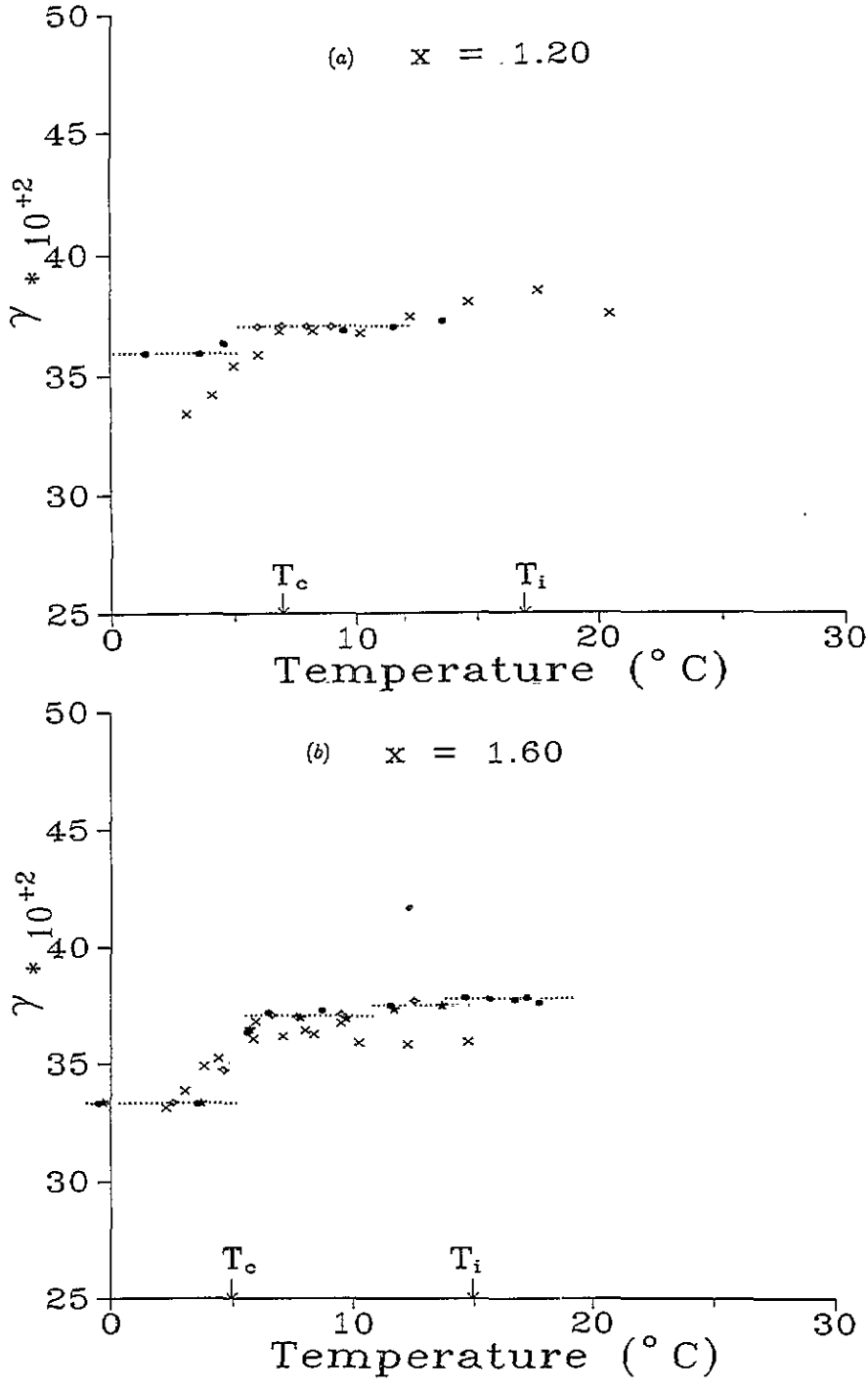

Figure 3. The size of the modulation wavevector $q = \gamma c^*$ as a function of temperature in $[(CH_3)_4N]_2ZnCl_{4-x}Br_x$. Full circles represent a first x-ray measurement, open circles a second one on the same crystal; ⋆ represents a second series of x-ray measurements on a second crystal and × morphological data from [9]. Arrows indicating T_i and T_c are from Colla *et al* [15, 16]. Plateaus of constant γ are indicated with a dotted line. The errors in γ are smaller than the size of the symbols used. (a) $x = 1.20$; (b) $x = 1.60$; (c) $x = 1.69$; (d) $x = 2.19$.

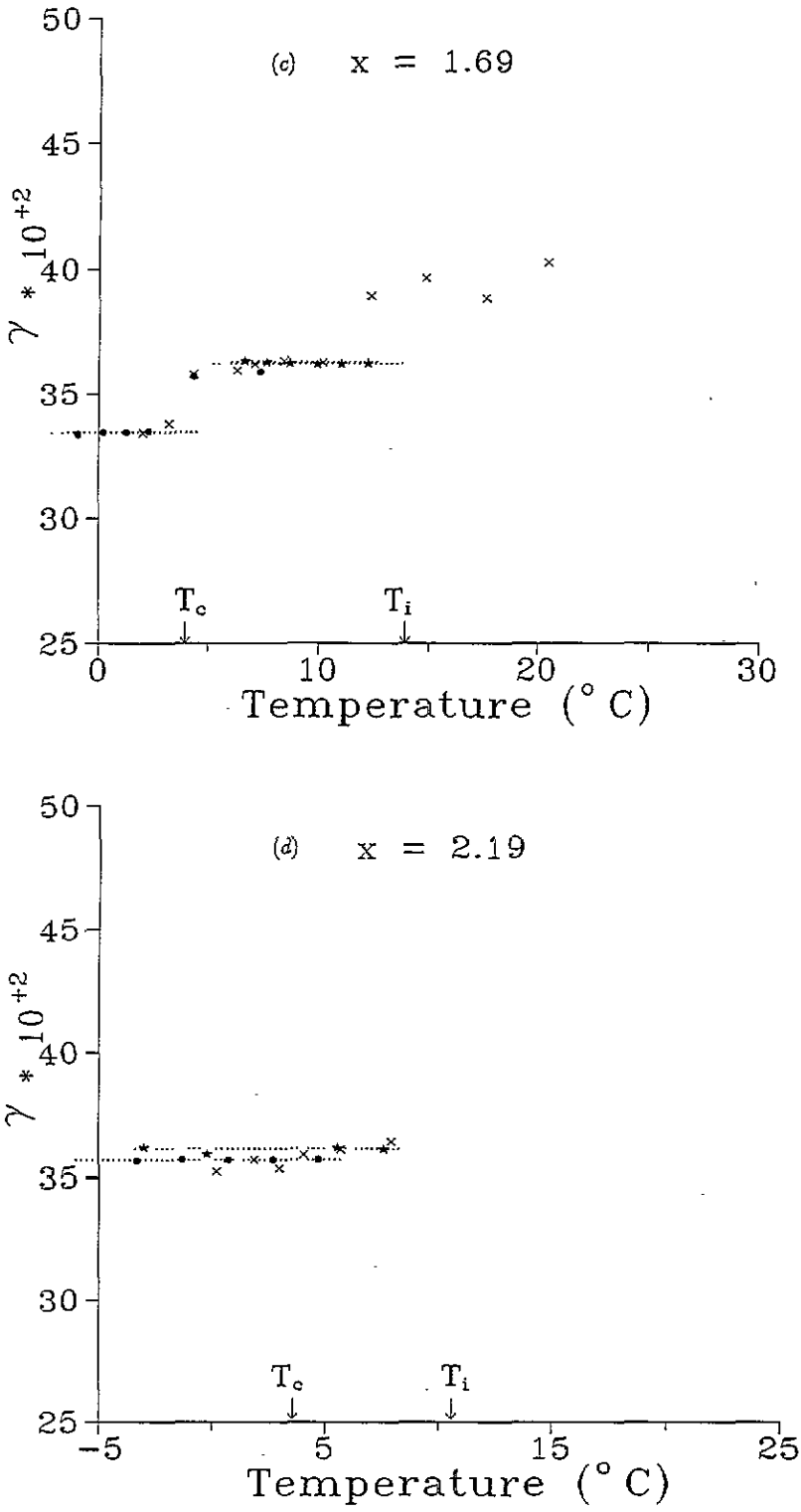

Figure 3. *(continued)*

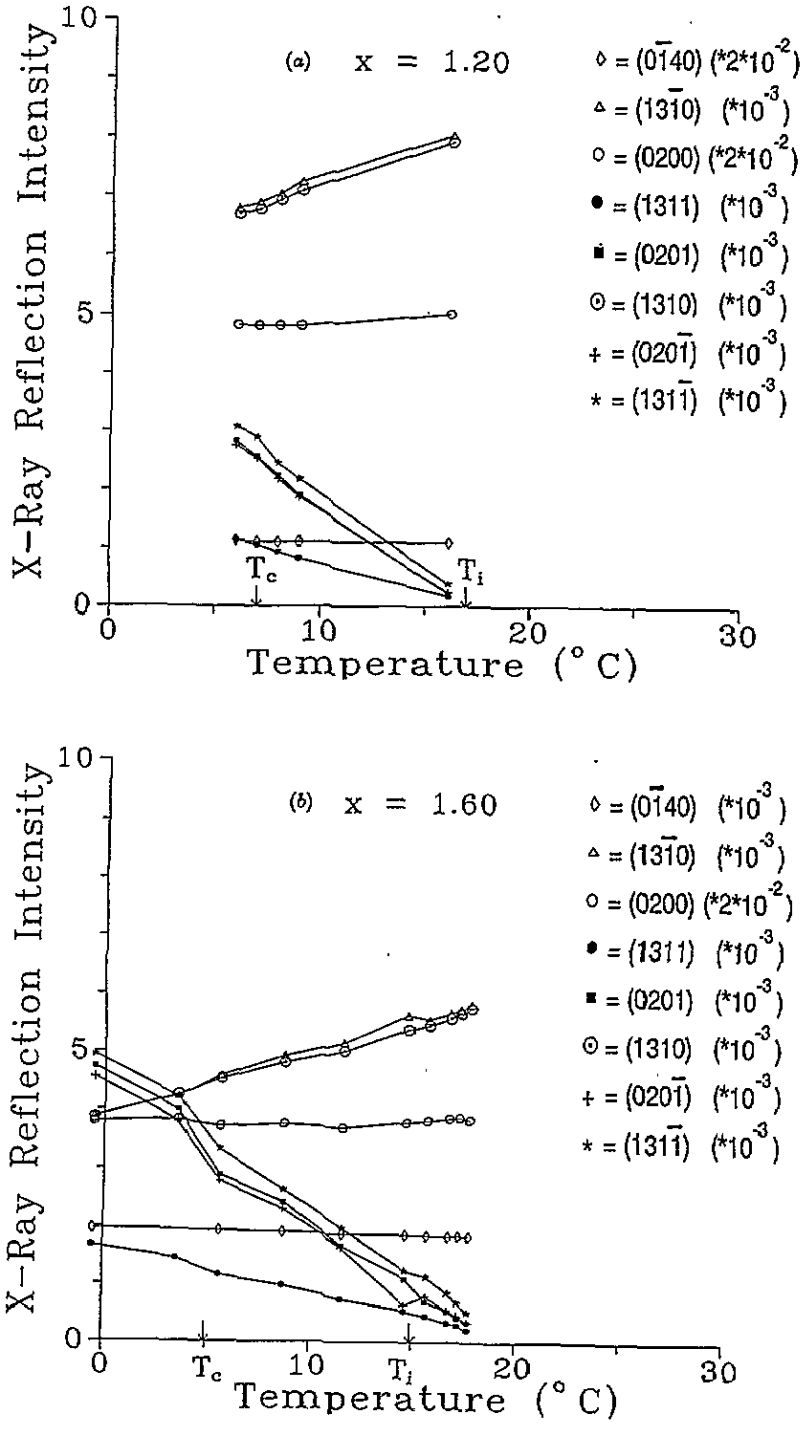

Figure 4. The intensity of main and satellite reflections as a function of temperature in $[(CH_3)_4N]_2ZnCl_{4-x}Br_x$ determined from x-ray measurements. All intensities are scaled to an interval of 0–10. Arrows indicating T_i and T_c are from Colla *et al* [15, 16]. The errors in the intensities are smaller than the size of the symbols used. (a) $x = 1.20$; (b) $x = 1.60$; (c) $x = 1.69$; (d) $x = 2.19$.

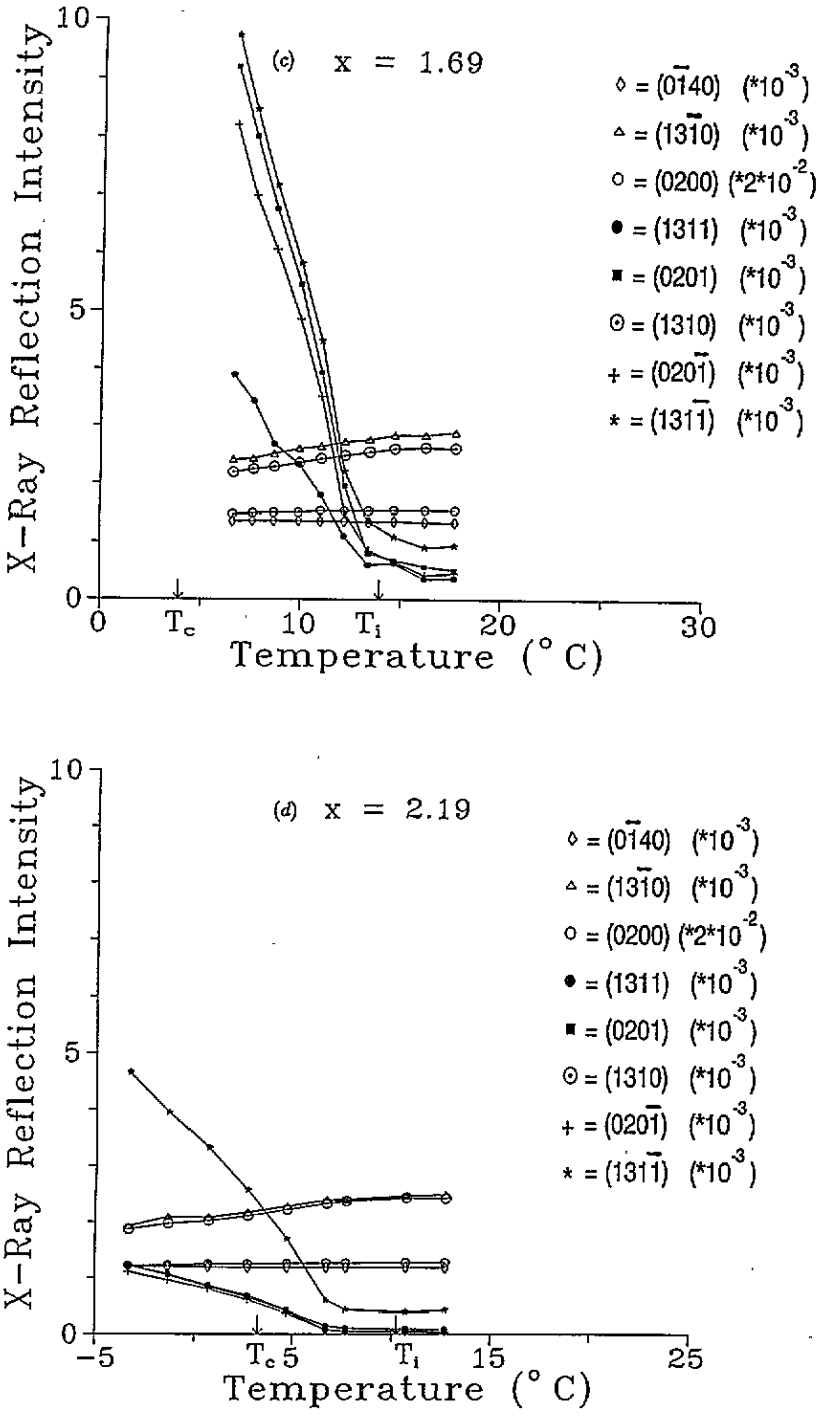

Figure 4. (*continued*)

Table 1. The observed plateaus in the values for γ for different compositions x. The corresponding temperature ranges are given. For the commensurate approximation of γ see the text.

$x = 0$		$x = 1.20$		$x = 1.60$		$x = 1.69$		$x = 2.19$	
T (°C)	γ	T (°C)	γ	T (°C)	γ	T (°C)	γ	T (°C)	γ
7.1–18.8	$\frac{5}{12}$ 0.4174 (±0.0021)	1.4–3.6	$\frac{14}{39}$ 0.3591 (±0.0036)	−0.5–3.7	$\frac{1}{3}$ 0.3336 (±0.0011)	−1.0–2.3	$\frac{1}{3}$ 0.3340 (±0.0012)	−3.3–4.7	$\frac{5}{14}$ or $\frac{16}{45}$ 0.3567 (±0.0007)
		6.0–11.6	$\frac{10}{27}$ 0.3702 (±0.0011)	6.7–9.5	$\frac{10}{27}$ 0.3705 (±0.0007)	6.6–7.6	$\frac{4}{11}$ 0.3632 (±0.0011)	−3.0–7.6	$\frac{13}{36}$ 0.3614 (±0.0014)
				11.6–17.7	$\frac{3}{8}$ 0.3753 (±0.0008)	8.7–12.2	$\frac{17}{47}$ 0.3620 (±0.0011)		
				14.7–17.2	$\frac{14}{37}$ or $\frac{17}{45}$ 0.3781 (±0.0011)				

4. Discussion

If we take the experimental errors into account—the morphological measurements have a larger uncertainty in the determination of γ (roughly ± 0.01); the x-ray measurements a larger uncertainty in the temperature determination—the results of the two experiments can be compared and show in general a large correlation. It should also be kept in mind that (apart from $x = 1.20$) at lower temperatures the data match better, while the main differences occur at higher temperature. As mentioned before the amplitude of the modulation decreases with T increasing towards the transition to the paraphase, resulting in a decrease of the intensity of the satellite reflections and of the stability of the satellite faces, and thus leading to a smaller accuracy in the experimental determination of γ.

If we take the modulation wave vector into consideration we observe a smooth change in γ for $x = 1.20$, with increasing temperature between the lock-in values. This also holds for $x = 1.60$, where lock-in phases are intermediated by incommensurate values for γ. For $x = 1.69$ the change in γ, especially from the lock-in phase of $\frac{1}{3}$ to that of $\frac{4}{11}$, seems to be somewhat less smooth. For $x = 2.19$ there are practically no changes in γ as a function of temperature, altough the two crystals show different values.

From both the satellite intensities and the variation in γ we are able to estimate T_i and T_c. For $x = 1.20$ T_i fits the data of Colla very well while no transition to the commensurate phase of $\gamma = \frac{1}{3}$ is found, as is suggested by the phase diagram of Colla [15]. For $x = 1.60$ T_c fits rather well, while T_i is considerably higher (± 20 °C, instead of 15 °C). For $x = 1.69$ T_i fits the data well, though T_c might be a bit higher. Here it is remarkable that the satellite intensities have very small remaining values for $T > T_i$. For $x = 2.19$ no clear phase transition can be observed, though the value for T_i is roughly correct.

It should be noted that when we regard the experimental results, the morphological experiment seems to be more sensitive to the modulation, as compared to x-ray experiments, because satellite forms are still observed at relatively higher temperatures in the incommensurate phase than satellite reflections. Whether this is due to the influence of the crystal surface, which is a crystallographic half plane and can therefore be regarded as an intrinsic defect, possibly stabilizing a commensurate value for the modulation, is not clear

at the moment. If the latter is relevant, this can also explain the remaining satellite reflection intensities in the paraphase. Another explanation for this remaining intensity can be found in the reported disorder in the orientation of the $ZnCl_4$ tetrahedra in the paraphase [25]. This disorder is probably related to the modulation in the incommensurate phase. The same structural disorder might explain the presence of satellite facets above T_i for $x = 1.20$ and $x = 1.69$. With the x-ray experiments we observed several stable values for the size of the modulation wave vector as can be found in table 1. The modulation wave vector shows some resemblance to a so-called devil's staircase as a function of temperature. The variation in γ on a plateau as we measured can easily be explained by experimental errors. The fact that we observe many lock-in phases makes us believe that small effects, e.g. defects, impurities, inhomogeneities in the ratio Cl/Br and the size of the crystal, easily 'pin' the modulation wavelength to a certain value. This also explains the relatively small energy differences between certain lock-in phases (with comparable γ). Furthermore memory effects play an essential role, because in some of the measurement runs on the same crystal, we found different lock-in values at comparable temperatures, although within a single run the value of γ almost always either increased or stayed constant with increasing temperature.

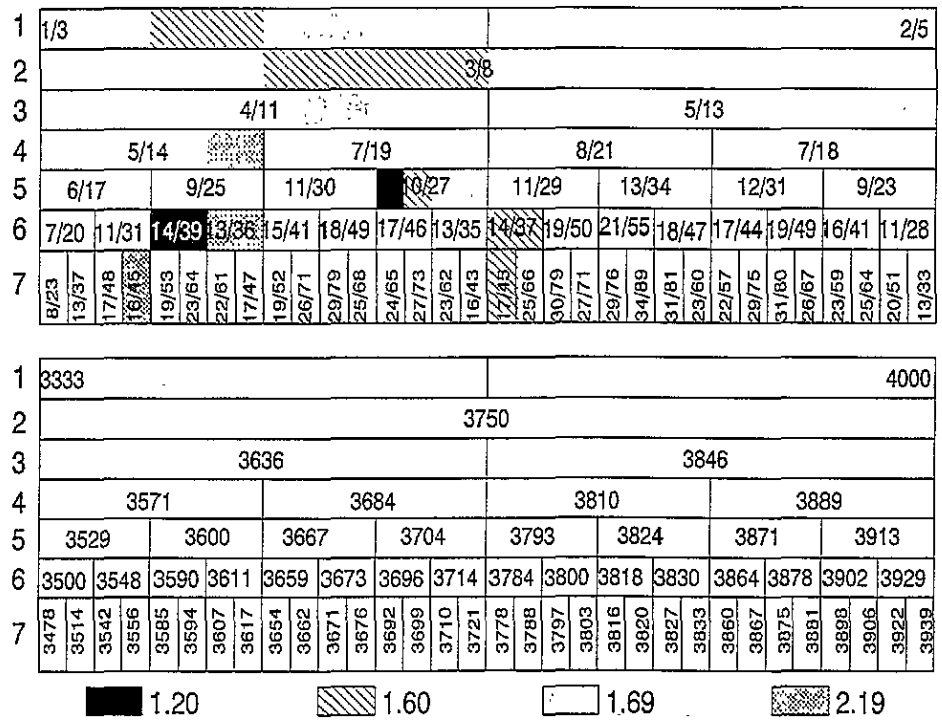

Figure 5. The first seven generations of Farey numbers starting from $\frac{1}{3}$ and $\frac{2}{5}$. Above: exact; below: decimal approximation. The different shaded areas represent the presence of the value in the measurements on the crystal with the indicated composition x.

Regarding the interpretation of the lock-in phases we can use the results of the microscopic model as discussed in the introduction in terms of the relevant series of Farey numbers. These series provide us with the possible values of the modulation wave vector describing the lock-in phases. We used the following procedure. First we determined the error in the measurement. Second we determined all possible Farey numbers of the two

relevant cases: the first where the 'boundary' phases were $\frac{1}{3}$ and $\frac{2}{5}$, the second where these phases were $\frac{2}{5}$ and $\frac{3}{7}$. The relevance of the starting values of the first series becomes clear if one looks at figure 1. Here, one sees that the incommensurate phase, and thus all phases lying within the incommensurate phase, for values $x > 0$ is bounded by a $\frac{1}{3}$ and a $\frac{2}{5}$ phase. The boundary due to the $\frac{0}{1}$ phase is not relevant as for our measurements ($x > 0$) the value of γ always is less than $\frac{2}{5}$. The boundary value $\frac{3}{7}$ of the second series is not present in figure 1, but it is in the unified phase diagram of Gesi [19, figure 9]. In all cases, the new phases 'emerge' from the two boundary phases, when the temperature and/or pressure is changed. We took the first seven generations of the Farey numbers, because this is sufficient to determine a value of the modulation wave parameter, lying within the experimental error, uniquely. The resulting series are given in figures 5 for $x > 0$ and 6 for $x = 0$. Third we evaluated all stable values for the wave vector, i.e. values that were more or less constant on a plateau over a temperature range of a few degrees celsius within a single experimental run, and chose the Farey number with the smallest integers n and m to describe this stable wave vector, with the value n/m lying within the experimental error. Of course it is possible to use further generations of the Farey numbers to obtain 'exactly' the experimental value, but, generally, this would imply relatively large values for n and m. The relevance of such large values like for example $m \geqslant 30$ can be questioned as it would imply a superstructure ordering consisting of thirty or more unit cells of the basic structure. Though not impossible, practical crystals contain many irregularities as discussed above so that such large values for the modulation wave vector are expected to be pinned down to smaller ones. On the other hand, it is then surprising that the value found experimentally is still well defined and does not cover a range of different values determined by the defect structure of the actual crystal.

In this way, we obtained for the crystals containing Br the values given in table 1. In figure 5 these values are indicated by different types of shading. It is not easy to find a correlation between the value of x (read pressure) and the presence of the different Farey numbers. In the case $x = 0$, the value of γ is always somewhat larger than $\frac{2}{5}$ and in that case the second series of Farey numbers is relevant (figure 6). Here we found a single stable value of $\frac{5}{12}$. In the phase diagram of Gesi, the region where the stable phase with $\gamma = \frac{3}{7}$ exists lies at pressures below the unified pressure of the $x = 0$ compound. Hence, the $\frac{5}{12}$ phase emerges from a phase which, though not present in the compound, still is reminiscent. The same commensurate value $\gamma = \frac{5}{12}$ was reported in $[(CH_3)_4N]_2ZnCl_4$ crystals which were irradiated with high-energy x-rays in order to induce defects [26]. The size of the $\frac{5}{12}$ plateau increased with the radiation exposure time.

5. Conclusions

Although the present investigation is far from complete, the results of our experiments indicate that it is possible to interpret measurements of the modulation wave vector in incommensurate crystal phases, showing different commensurate subphases, in terms of the microscopic model mentioned. Besides a confirmation of the presence of the morphologically found $\gamma = \frac{4}{11}$ commensurate phases in $[(CH_3)_4N]_2ZnCl_{4-x}Br_x$ we found some seven other commensurate phases stable in small but finite temperature ranges. Although the indexing of the corresponding modulation wave vectors is not unique, especially when one allows large supercells, we chose an indexing based on Farey numbers resulting from the microscopic one-dimensional frustrated ϕ^4 model worked out by Janssen and Tjon. This model fits very well in the unified description of Gesi. It would therefore be

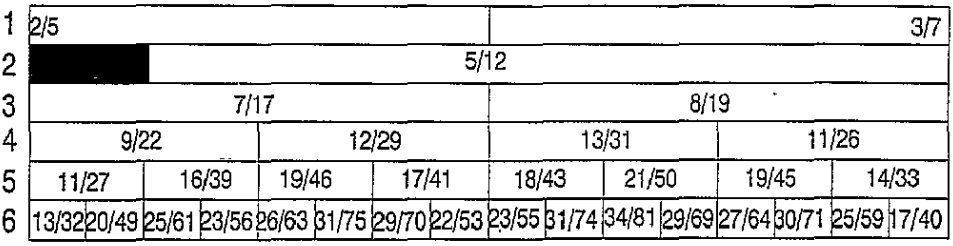

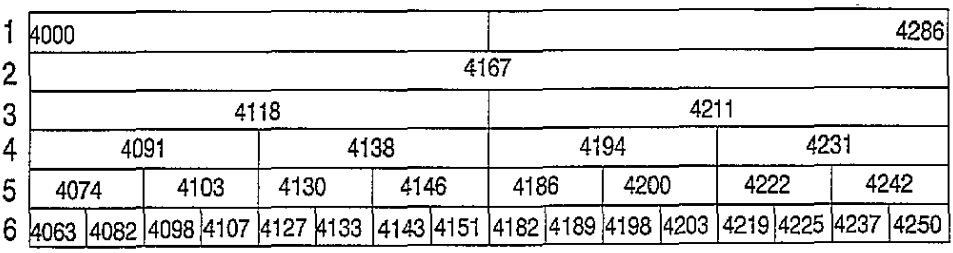

Figure 6. As figure 5, but now with starting values $\frac{2}{5}$ and $\frac{3}{7}$, which are relevant for the composition $x = 0$.

interesting to study the presence of commensurate phases within this unified phase diagram also experimentally in more detail, especially within the incommensurate phases of crystals with an average β-K_2SO_4 structure. As it is, however, known that defects in this type of crystals can result in metastable lock-in phases, this aspect will also have to be taken into account in such investigations.

6. Acknowledgment

One of the authors acknowledges the financial support of the Netherlands Organization for Scientific Research (NWO/SON project No 700-332-012).

References

[1] de Wolff P M 1977 *Acta Crystallogr.* A **33** 493
[2] Janner A and Janssen T 1977 *Phys. Rev.* B **15** 643
[3] Janner A and Janssen T 1980 *Acta Crystallogr.* A **36** 399, 408
[4] Janssen T and Janner A 1987 *Adv. Phys.* **36** 519
[5] Janner A, Rasing Th, Bennema P and van der Linden W H 1980 *Phys. Rev. Lett.* **45** 1700
[6] Dam B and Janner A 1986 *Acta Crystallogr.* B **42** 69
[7] Dam B and Janner A 1983 *Z. Kristallogr.* **165** 247
[8] Dam B 1985 *Phys. Rev. Lett.* **55** 2806
[9] Vogels L P J, Verheijen M A, Meekes H and Bennema P 1992 *J. Cryst. Growth* **121** 697
[10] Bennema P, Balzuweit K, Dam B, Meekes H, Verheijen M A and Vogels L P J 1991 J. *Phys. D: Appl. Phys.* **24** 186
[11] Wiesner J R, Srivastava R C, Kennard C H L, Di Vaira M and Lingafelter E C 1967 *Acta Crystallogr.* **23** 565

[12] de Wolff P M, Janssen T and Janner A 1981 *Acta Crystallogr.* A **37** 625
[13] Trouélan P, Lefebvre J and Derollez P 1984 *Acta Crystallogr.* C **40** 386
[14] Tanisaki S and Mashiyama H 1980 *J. Phys. Soc. Japan Lett.* **48** 339
[15] Colla E L 1987 *Thesis* Swiss Federal Institute of Technology, Zürich
[16] Colla E, Gramlich V and Petter W 1987 *Acta Crystallogr.* C **43** 1070
[17] Madariaga G, Zuñiga F J, Pérez-Mato J M and Tello M J 1987 *Acta Crystallogr.* B **43** 356
[18] Janssen T 1986 *Ferroelectrics* **66** 203
[19] Gesi K 1986 *Ferroelectrics* **66** 269
[20] Elliott R J 1961 *Phys. Rev.* **124** 346
[21] Selke W 1984 *Modulated Structure Materials* ed T Tsakalakos (Dordrecht: Nijhoff) p 23
[22] Janssen T and Tjon J A 1982 *Phys. Rev.* B **25** 3767
[23] Selke W and Duxbury P M 1984 *Z. Phys.* B **57** 49
[24] Hoogervorst A C R 1986 *Thesis* Delft University of Technology
[25] Itoh K, Hinasada A, Matsunaga H and Nakamura E 1983 *J. Phys. Soc. Japan* **52** 664
[26] Bziouet M, Almairac R and Saint-Grégoire P 1987 *J. Phys. C: Solid State Phys.* **20** 2635